References

[1] Wen, S. and Chi, L.K., "Higher-order Asymptotic Solutions to the Bhatnagar-Gross-Krook Equation," *The Physics of Fluids*, Vol. 18, 1975, pp. 387-388.

[2] Chi, L.K., "Asymptotic Solutions of the Bhatnagar-Gross-Krook Equation," *The Physics of Fluids*, Vol. 8, 1965, pp. 991-992.

[3] von Karman, Th., "The Engineer Grapples with Non-linear Problems," *Bulletin of the American Mathematical Society*, Vol. 46, 1940, pp. 615-683 (in particular pp. 655-659).

[4] Blasius, H., "Grenzschichten in Flussigkeiten mit kleiner Reibung," *Zeitschrift fuer Angewandte Mathematik und Physik*, Vol. 56, 1908, pp. 4-13.

[5] Topher, C., Bemerkungen zu dem Aufsatz von H. Blasius, "Grenzschichten in Flussigkeiten mit Kleiner Reibung," *Zeitschrift fuer Angewandte Mathematik und Physik*, Vol. 60, 1912, pp. 397-398.

[6] Goldstein, S., *Modern Developments in Fluid Dynamics*, Vol. I, Oxford University Press, 1938, pp. 135-137.

[7] Alden, H.L., "Second Approximation to the Laminar Boundary Layer Flow Over a Flat Plate," *Journal of Mathematics and Physics*, Vol. 27, 1948, pp. 91-104.

[8] Goldstein, S., "Flow of an Incompressible Viscous Fluid Along a Semi-infinite Flat Plate," Engineering Research Institute, University of California, Tech. Rept. HE-150-144, 1956.

[9] Imai, I., "Second Approximation to the Laminar Boundary-Layer Flow Over a Flat Plate," *Journal of the Aeronautical Sciences*, Vol. 24, 1957, pp. 155-156.

[10] Goldstein, S., *Lectures on Fluid Mechanics*, Wiley, New York, 1960, pp. 115-144.

[11] Van Dyke, M., *Peturbation Methods in Fluid Mechanics*, Annotated Edition, The Parabolic Press, Stanford, Calif., 1975, pp. 121-147, 230-232.

Axisymmetric Calculations of Transonic Wind Tunnel Interference in Slotted Test Sections

K.R. Karlsson* and Y.C.-J. Sedin†
SAAB-SCANIA AB Aerospace Division, Linköping, Sweden

Nomenclature

a = slot width
C_p = $(p-p_\infty)/\rho_\infty U_\infty^2/2$, normalized pressure coefficient
$\mathfrak{F}$ = wall b.c. functional, Eq. (1)
F = $r\bar{\varphi}_r$, Eq. (3)
G = $\bar{\varphi}-\ell n(r)\cdot F$, Eq. (3)
l = slot depth
M_∞ = Mach number of reference flow
N = number of slots
p = pressure
p_p = pressure in plenum chamber
p_∞ = pressure in reference flow
q = slot flux/unit length
Q = normalized slot flow potential, Ref. 1
r = radius vector in cross-flow plane
U_∞ = velocity in reference flow
v = normalized slot velocity at y_p, Ref. 1
x = distance along tunnel axis
y_p = coordinate of line in slot center plane where the plenum pressure is imposed, $y_p=0$ at the slot entrance; Ref. 1
γ = specific heat ratio
δ = $(p_p-p_\infty)/\rho_\infty U_\infty^2$; normalized plenum pressure
$\bar{\varphi}$ = perturbation velocity potential to approximate problem, Eq. (2)
$\bar{\varphi}_0$ = integration constant given at beginning of slot, Eq. (6)
ρ_∞ = density of reference flow
FTI = figure of tunnel interference, Eq. (7)

Received March 5, 1979.

Index categories: Testing, Flight and Ground; Computational Methods; Research Facilities and Instrumentation.

*Research Engineer. Systems Development Laboratory.

†Senior Research Engineer. Department of Aerodynamics. Member AIAA.

Introduction

WIND tunnel interference poses a serious problem when testing models in the transonic speed regime. One way to avoid this problem is to use comparatively small models. However, small models will usually yield Reynolds numbers that are too low and large test sections will give too expensive tunnels. A numerical method is urgently required to help resolve these conflicting interests. Recently, a theory for slotted test sections was presented by Berndt.[1] A study has been commenced to investigate numerically the consequences of this theory, and some of the very first results are presented herein. Up to now, only axisymmetric flows have been calculated, although this is no limit to the theory. The wall interference on the model has been defined through a single number, called the figure of tunnel interference (FTI). The FTI is based on an average value of the difference in model surface pressure between the tunnel case and the simulated freestream case. Two different tunnel blocking ratios are demonstrated for a parabolic arc body mounted on a sting at two different Mach numbers, the higher of which gives a fully choked test section. The present calculations only cover test sections with slots of constant width. However, work is now going on with varying slot widths in an attempt to find slot shapes that, hopefully, will give an almost interference-free flow in the test section.

General Outlines of the Theory

The theory of Ref. 1 is built on the calculation of an approximate velocity perturbation potential $\bar{\varphi}$. In comparison with the "exact" solution φ, the approximate $\bar{\varphi}$ is created by averaging (filtering) φ with respect to higher order crossflow variations, caused by the slots and the walls in the test section. By using slender-body cross-flow theory in combination with matched asymptotic expansions, the slot flow is coupled to the averaged potential through a pressure balance equation for each slot. The line y_p along which the plenum pressure δ is specified for each slot is a priori unknown and therefore a part of the total solution. The aforementioned coupling results in a homogeneous wall boundary condition for each slot, giving a relation between $\bar{\varphi}$ and the radial velocity $\bar{\varphi}_r$:

$$\bar{\varphi}=\mathfrak{F}(\bar{\varphi}_r) \tag{1}$$

The functional $\mathfrak{F}$ in Eq. (1) includes the dependence on geometrical data such as the slot width $a(x)$, the depth l, and the number of slots N, as well as the plenum pressure δ. In the general case, a trigonometric interpolation is needed between slots to give the complete outer boundary condition for $\bar{\varphi}$ at the wall surface. The inner boundary condition is the usual slender-body-type approximation of the tangency flow condition, which in the axisymmetric case specifies $r\bar{\varphi}_r$ close to the x axis. At the entrance of the test section, values of $\bar{\varphi}_x$ are coupled to the plenum pressure coefficient, which gives the entrance Mach number. The nonlinear problem for $\bar{\varphi}$ is solved by numerically iterating on the transonic small-perturbation equation between the model and the tunnel wall, repeatedly using relation (1) as an outer wall condition.

Basic Equations and Numerical Procedures

The axisymmetric potential equation is given by

$$[(1-M_\infty^2)-M_\infty^2(\gamma+1)\bar{\varphi}_x]\bar{\varphi}_{xx}+(r\bar{\varphi}_r)_r/r=0 \tag{2}$$

The reference flow, which the tunnel test is supposed to simulate in the neighborhood of the model, is the desired freestream case with Mach number M_∞. In Refs. 2 and 3 a rapid finite-difference method was presented for solving transonic flow problems in cylindrical coordinates. This method decomposes the potential into two new functions F and G so that $F=r\bar{\varphi}_r$ and $G=\bar{\varphi}-\ell n(r)\cdot F$. These definitions, together with Eq. (2), will give the system

$$\begin{aligned} F_r &= -r[1-M_\infty^2-M_\infty^2(\gamma+1)\bar{\varphi}_x][\ell n(r)\cdot F_{xx}+G_{xx}] \\ G_r &= r\ell n(r)\cdot[1-M_\infty^2-M_\infty^2(\gamma+1)\bar{\varphi}_x][G_{xx}+\ell n(r)\cdot F_{xx}] \end{aligned} \tag{3}$$

Equations (3) are solved separately in an iterative manner, repeatedly going outward with F and inward with G. Initial values of F are given by the model geometry close to $r=0$ and starting values of G are provided by solving relation (1), so that $G=\mathfrak{F}(F)$ at the chosen tunnel radius, $r=1$. The upstream and downstream conditions are given by $\bar{\varphi}_x=-\delta$ and $\bar{\varphi}_{xx}=0$, respectively. In the axisymmetric case, with a cylindrical test section ($r=1$) provided with N equal and uniformly distributed slots of constant width a, the wall condition, Eq. (1), symbolizes the solution of the following set of equations

$$q=2\pi\cdot\bar{\varphi}_r(x,1)/N \tag{4}$$

$$dy_p/dx=qv/a \tag{5}$$

$$d/dx[\bar{\varphi}-\bar{\varphi}_0+q(Q-\ell n(Na)/\pi)]+(qv/a)^2/2+\delta=0 \tag{6}$$

The variable q denotes the flux through each slot and $y_p(x)$ is the line in the center plane of the slot, where the plenum chamber pressure δ is specified. Equation (6) expresses the pressure balance along $y_p(x)$ and contains a quadratic cross-flow term. v and Q are the normalized velocity and velocity potential functions for an isolated slot of unit width and unit flux. For further details about the slot flow model, see Ref. 1. A typical finite-difference mesh divides the test section into 60×40 points in the x and r-directions, respectively. About 20 x-points cover the body. The test section has a typical length of about 3 tunnel radii. The tunnel interference is quantified by the figure of tunnel interference (FTI) according to the sum

$$\mathrm{FTI}=\left(\sum_{i=1}^{n}(\Delta C_p)_i^2/n\right)^{1/2}\Big/|C_{p_{\min}}| \tag{7}$$

Equation (7) is evaluated over the surface of the body and ΔC_p is the pressure coefficient difference between the tunnel run and the desired freestream case. $|C_{p_{\min}}|$ is the absolute value of the minimum pressure, which corresponds to the maximum velocity in the freestream case and n denotes the number of mesh points covering the body.

Results and Discussions

Figures 1-3 show some calculated results. In all cases, the "tested" model is a parabolic arc of revolution. The fineness ratio is $6\sqrt{2}$ based on the full body length. The body-sting junction is at 5/6 of the full length. Thus, the actual body length is equal to the tunnel radius when the blocking ratio, defined as the maximum model cross-sectional area to the tunnel cross-sectional area, is 0.5%. All figures presented apply to a test section with 8 uniformly distributed slots. The upper part of Fig. 1 shows the FTI as a function of the wall ventilation at two different Mach numbers and two blocking

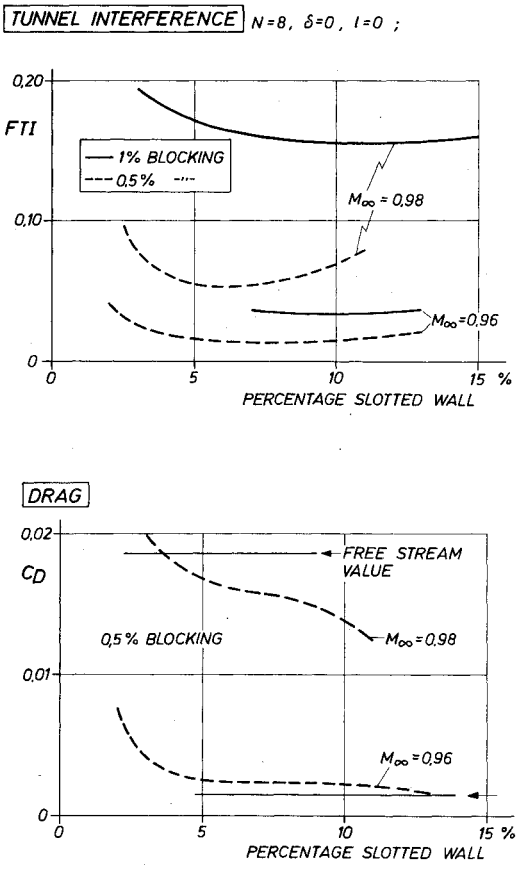

Fig. 1 Tunnel interference and pressure drag as functions of slot width.

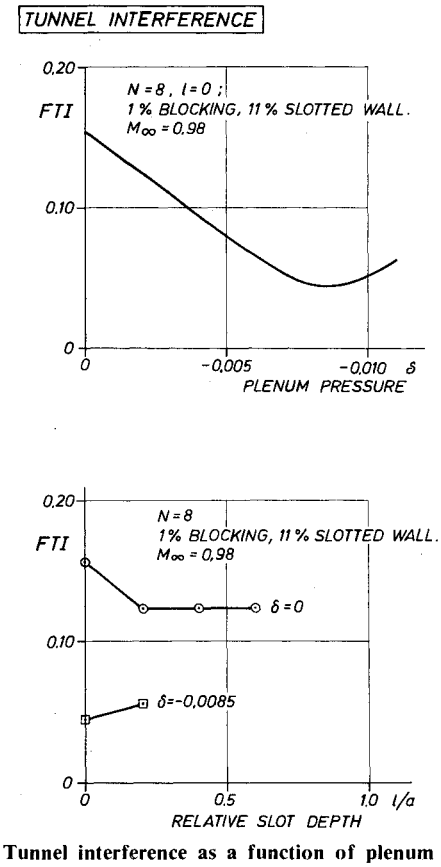

Fig. 2 Tunnel interference as a function of plenum pressure and relative slot depth.

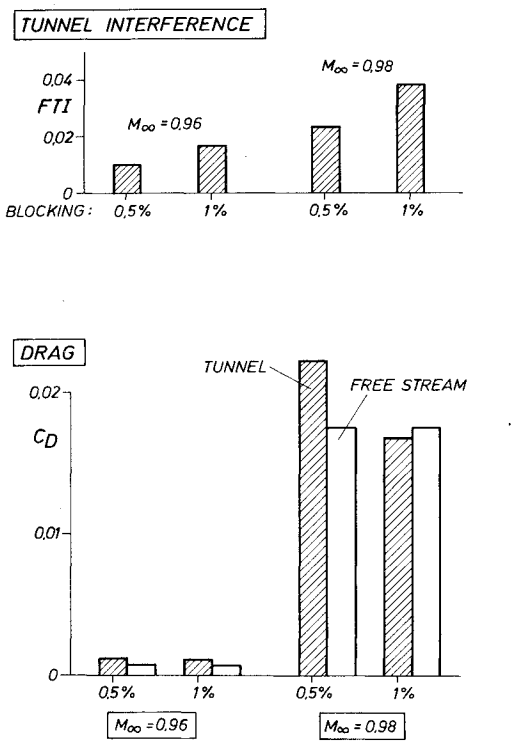

Fig. 3 Typical levels of interference and corresponding pressure drag, realized by searching for "optimal" parameter settings.

ratios (0.5%, 1%). The corresponding inviscid pressure drag of the 0.5% case is shown in the lower part of Fig. 1. It is interesting to note that the drag inflexion points coincide with the minimum FTI. The plenum pressure is zero in Fig. 1, which sets the entrance Mach number to M_∞. The tunnel is fully choked for $M_\infty = 0.98$ while $M_\infty = 0.96$ is at the beginning of the drag-rise phase.

Figure 2 shows what happens to the FTI when the plenum pressure δ and the relative slot depth l/a are varied at $M_\infty = 0.98$ for the 1% area blocking case. The ventilation is the optimal 11% found in Fig. 1. The tunnel interference is considerably reduced by increasing the plenum suction. From Fig. 2 it can be concluded that $\delta = -0.0085$ and 11% ventilation is an "optimal" setting for zero slot depth. This plenum pressure corresponds to an entrance Mach number of 0.99. Figure 3 gives typical examples of the magnitudes to which the tunnel interference can be reduced, when searching for optimal parameter settings for different blocking ratios. It is perhaps paradoxical that the tunnel drag differs more from the reference drag in the 0.5% blocking case than in the 1% case. However, this depends on how the model surface pressures in the two cases are distributed over the body. It should be pointed out that the drag algorithm used in Fig. 3 was improved compared to that applied in Fig. 1. However, the main impression was not altered by this. Work is now ongoing to inversely design slot shapes of varying width that will give almost zero interference on the model. So far, the results are promising and indications are that the tunnel wall boundary layer might play an important role in this.

References

[1] Berndt, S.B., "Inviscid Theory of Wall Interference in Slotted Test Sections," *AIAA Journal*, Vol. 15, Sept. 1977, pp. 1278-1287.

[2] Sedin, Y.C.-J., "Axisymmetric Sonic Flow Computed by a Numerical Method Applied to Slender Bodies," *AIAA Journal*, Vol. 13, April 1975, pp. 504-511.

[3] Karlsson, K.R. and Sedin, Y.C.-J., "The Method of Decomposition Applied in Transonic Flow Calculations," *Lecture Notes in Physics*, Vol. 59, Springer Verlag, New York, 1976, pp. 262-267.

Generalized Velocities in the Outer Region of Hypersonic Turbulent Boundary Layers

Ralph D. Watson*
NASA Langley Research Center, Hampton, Va.

Nomenclature

C = constant in law of the wall, Eq. (2)
k = mixing length slope near wall
R_θ = Reynolds number based on momentum thickness
T = temperature
u = velocity
u^* = generalized velocity [see Eq. (1)], or incompressible velocity
u_τ = shear velocity, $(\tau_w/\rho_w)^{1/2}$
w = wake function, Eq. (4)
y = distance from surface
δ = boundary-layer thickness from pitot survey
η = y/δ_c
ν = kinematic viscosity
Π = velocity defect constant
ρ = density
τ = shear stress

Subscripts

c = edge of wake region
e = edge of boundary layer
w = at wall
t = stagnation value

THE transformation of a compressible turbulent boundary layer to its incompressible counterpart has been studied for many years, primarily to determine the surface shear stress from the velocity profile without resorting to tedious skin friction balance measurements. Boundary-layer transformations are of two types—one in which the y coordinate is modified by Howarth-Dorodnitsyn scaling; the other in which the compressible velocity profile is modified by a density scaling. Many y coordinate transformations are based on Coles' work in Ref. 1, while velocity transformations often stem from Van Driest's mixing length analysis in Ref. 2. A review of both types of transformations, along with extensive references for each, can be found in Ref. 3. The purpose of this Note is to show that the outer portion of the velocity profile of hypersonic turbulent boundary layers can be transformed so that the constants determined by a best fit to the law of the wake[4] are in reasonable agreement with the wake constant for incompressible boundary layers at the same Reynolds number.

Both y transformations and velocity transformations produce velocity profiles which, with the proper choice of τ_w to give u_τ, can be reduced to the incompressible law of the wall. For example, the y transformation of Ref. 5 adequately transformed both adiabatic and cold wall velocity profiles in the wall region for Mach numbers up to about 9. Skin friction coefficients obtained by fitting transformed profiles to the incompressible flow law of the wall were generally in good

Received Aug. 11, 1978; revision received March 5, 1979. This paper is declared a work of the U.S. Government and therefore is in the public domain.

Index category: Boundary Layers and Convective Heat Transfer—Turbulent.

*Aerospace Engineer, Fluid Mechanics Branch, High Speed Aerodynamics Division. Member AIAA.